Single Crystal Diffraction Studies of WO$_3$ at High Pressures and the Structure of a High-Pressure WO$_3$ Phase

Y. Xu, S. Carlson, and R. Norrestam[1]

Structural Chemistry, Arrhenius Laboratory, Stockholm University, S-10691 Stockholm, Sweeden

The structural changes of crystalline WO$_3$ induced by the changes in pressure from ambient pressure up to 47 kbar have been studied with a diamond anvil cell. The investigations have been performed by single crystal X-ray diffraction techniques using MoKα radiation. The results obtained show that triclinic WO$_3$, considered to be the thermodynamically stable form at ambient pressure, undergoes a reversible phase transition already in the range 0.3–1.2 kbar to give a monoclinic high-pressure (HP) form with a halved unit cell volume. The pressure transition, is expected as a consequence of the fact that the pseudo-C-centered lattice of the triclinic phase becomes a true lattice symmetry when the pressure is increased. Atomic displacements of only a few tenths of an Å are involved in the transition. These observations agree in general with the results previously obtained by E. Salje and G. Hoppmann from their studies of the Raman spectra of WO$_3$ at high pressure. (1980 *High Temp. High Pressure* **12,** 213–216. The HP phase has the space group symmetry $P2_1/c$, with $a = 5.261(1)$, $b = 5.128(1)$, $c = 7.650(4)$ Å, and $\beta = 92.05(3)°$ at 5.7 kbar. The compressibility of the HP phase is largest along the [010] direction. The isothermal bulk modulus, $B_0 = 44.5(9)$ GPa, at ambient pressure and its derivative, $B_0' = 2.5(4)$, were determined by least squares techniques using the Birch equation of state. Apart from the general decrease in the cell parameters when the pressure was increased to 47 kbar, no apparent symmetry changes were detected. Thus, the monoclinic HP form appears to be the stable form in the investigated pressure range. Single crystal diffraction data of the HP form at 5.7 kbar were collected and a derived structure model was refined *versus* 227 reflection amplitudes to an R value of 0.040. The 3 + 3 coordination around W is more pronounced in the HP structure (three shorter bonds of 1.78 to 1.84 Å and three longer bonds of 2.02 to 2.14 Å) than in that at ambient pressure. The phase transition involves a significant change of the W positions relative to the centroids of the coordination octahedra. © 1997 Academic Press

INTRODUCTION

Crystalline WO$_3$ has been reported to adopt several different symmetries (e.g., triclinic, monoclinic, orthorhombic,

tetragonal, hexagonal) with increasing temperature. Two modifications, sometimes denoted WO$_3$(I) and WO$_3$(II), are reported to exist at ambient conditions (2), WO$_3$(I) being monoclinic, space group $P2_1/n$ with $a = 7.301$, $b = 7.539$, $c = 7.690$ Å, and $\beta = 90.89°$, and WO$_3$(II) being triclinic, space group $P\bar{1}$, with similar cell dimensions, viz. $a = 7.313$, $b = 7.525$, $c = 7.689$ Å, $\alpha = 88.85$, $\beta = 90.91$, and $\gamma = 90.94°$. Both of these phases have been found (3) to undergo first-order transitions (at $-50°$C and at $-27°$C, respectively) to a low-temperature phase with the monoclinic space group symmetry Pc and unit cell parameters $a = 5.275$, $b = 5.155$, $c = 7.672$ Å, and $\beta = 91.7°$. The triclinic WO$_3$(II) structure (2, 4, 5), is considered to be the thermodynamically stable form at ambient temperature and pressure. Most of the other low- and high-temperature WO$_3$ modifications have structures closely related to this triclinic form. The oxygen coordination around the W atoms in WO$_3$ has a strongly distorted octahedral geometry. The coordination octahedra share all six corners with other octahedra to form a three-dimensional structure of ReO$_3$ type (6).

The structure of the triclinic WO$_3$(II) has a pronounced pseudo-symmetry. With regards to, e.g., the W positions, the numerical deviations of the fractional coordinates from a pseudo-monoclinic $P2_1/n$ are rather small. This monoclinic symmetry would relate the position (cf. 4) of the W(1) atom with fractional coordinates (0.257, 0.026, 0.285) to that of W(2) at (0.250, 0.528, 0.216) and the position of W(3) at (0.244, 0.031, 0.782) to that of W(4) at (0.250, 0.534, 0.719) via the pseudo-symmetry operation $(x, y, z) \rightarrow (\frac{1}{2} - x, \frac{1}{2} + y, \frac{1}{2} - z)$. The deviation in fractional coordinates when this operation is applied to these positions is thus less than (0.004, 0.002, 0.001) or just a few hundreds of an Å. A transition from the triclinic to this monoclinic space group has to involve both very small changes of the W positions and a small change of the packing pattern to give a monoclinic unit cell having $\alpha = \gamma = 90°$. The small changes needed are likely to explain the reported coexistence of the triclinic WO$_3$(II) and monoclinic WO$_3$(I) form under ambient conditions.

The $WO_3(II)$ structure can, on the other hand, also be regarded as pseudo-C-centered; viz. a primitive subcell with half the volume of the triclinic cell can also be used to describe the structure. The unit cell of the subcell would have the dimensions $a \approx 5.3$, $b \approx 5.2$, $c \approx 7.7$ Å and $\alpha \approx \beta \approx \gamma \approx 90°$. The pseudo-centering would relate the position of W(1) at fractional coordinates (0.257, 0.026, 0.285) to those of W(4) at ($\frac{1}{2} + 0.250$, $\frac{1}{2} - 0.034$, 0.281) and the position of W(2) at (0.250, 0.528, 0.216) to that of W(3) at ($\frac{1}{2} + 0.256$, $\frac{1}{2} - 0.031$, 0.218). The deviation, when the C-center operation was applied, on the W atomic positions would then be less than (0.004, 0.030, 0.002); viz the largest deviation (about 0.2 Å) occurs along [010] of the triclinic cell. The magnitude of this deviation is thus an order of magnitude larger than the deviation between the $WO_3(II)$ and the $WO_3(I)$ structures discussed above. Despite the larger changes involved (a few tenths of an Å), it appears reasonable to anticipate that a transition from the triclinic form to a structure with a halved unit cell volume could occur under nonambient conditions. In fact, a low-temperature phase with monoclinic space group symmetry Pc and with the unit cell dimensions $a = 5.275$, $b = 5.155$, $c = 7.672$ Å, and $\beta = 91.7°$ was reported by Salje in 1976 (3). Unfortunately, the poor crystal quality prohibited any single crystal diffraction study to be carried out that would fully characterize this WO_3 phase. As one of the referees pointed out to us, Salje and Hoppman in 1980 (1) have also performed high-pressure investigations of WO_3 up to about 14 kbar, with spectroscopic (Raman) and photographic X-ray (Laue) methods.

The present investigation was undertaken to obtain information on the behavior of WO_3 under moderate pressures up to 50 kbar. With the synthetic procedures applied (cf. below), well-defined nontwinned single crystals were obtained only for triclinic $WO_3(II)$. The unit cell parameters determined by single crystal diffractometry for selected crystals were within $3 \cdot \sigma$ from those given by Woodward *et al.* (2). As no nontwinned crystals were obtained for the monoclinic $WO_3(I)$ form, the present investigation was confined to studies of the influence of pressure on the triclinic $WO_3(II)$ modification.

The investigation is part of a research program aimed at high-pressure X-ray diffraction studies of simple oxides and fluorides. A short report on these studies was given at the recent crystallography conference, IUCr XVIII, in Seattle in August 1996 (7).

EXPERIMENTAL

Synthesis. Crystalline triclinic $WO_3(II)$ was prepared by inserting one end of a long (55 cm) silica tube, containing WO_3 (Johnson Matthey, Puratronic powder 99.998%), into a furnace running at 1350°C for 24 h under oxygen atmosphere. Quartz wool was inserted into the other end of the tube. The temperature was then lowered to ambient temperature with a speed of 1°/min. The specimens obtained were characterized by Guinier X-ray powder techniques and by EDS analyses using a SEM microscope. The powder patterns were consistent with that of $WO_3(II)$, and no significant amounts of any contaminating elements were found. Single crystal photographic techniques (de Jong and precession methods) were utilized to select well-defined nontwinned single crystals suitable for the subsequent high-temperature studies.

High-pressure X-ray studies. The single crystal high-pressure studies were carried out with a Merril–Bassett-type diamond anvil cell (Diacell Products DXR-5 cell), having top diamond face diameters of 600 μm. A methanol–ethanol–water mixture (16:3:1) was used as a pressure transmitting medium. Cold-rolled stainless steel foils (type SS 142331-44), 400 μm thick, were used as gasket materials. Centered holes with diameters of 300 μm were drilled mechanically in preindented gaskets using a simple, in-house designed, drilling jig equipment.

Pressure was monitored by measuring the wavelength shift of the ruby fluorescence line at 6941 Å from small ruby crystals (< 20 μm) inserted into the pressure cell. A linear shift was assumed to be valid within the studied pressure range and the proportionality constant used was 2.74 kbar $Å^{-1}$ (8). The wavelength shifts were measured with "home-assembled" equipment consisting of *inter alia* a 25 mW Ar ion laser and a spectrograph (Oriel Multispec) equipped with a 1024 diode array detector controlled by a PC computer. Pressure was monitored immediately before and after the diffractometer investigations.

Single crystal unit cell data and X-ray intensity data for crystals inside the high-pressure diamond anvil cell (DAC) were collected with a four-circle diffractometer (Siemens P4/RA). The diffractometer was equipped with a high-speed scintillation detector (Siemens FSD), using graphite monochromatized $MoK\alpha$ radiation ($\lambda = 0.71073$ Å) from a rotating anode generator (Siemens M18XHF). The generator was operated at 5.0 kW (50 kV and 100 mA) for a filament size of 0.3×3 mm and a collimator with the diameter $\phi_i = 350$ μm. Unit cell parameters were determined by least squares fitting to the angular settings of 17 well-centered single crystal reflections. Pressures, monitored before and after each determination of the cell parameters, deviated by less than 0.3 kbar.

Single crystal X-ray diffraction data were collected for those reflections with $2\theta < 80°$, which could be expected to not be completely absorbed by the DAC hardware. Intensities were measured by applying $\omega, 2\theta$ scans at azimuthal angles (ψ) selected to minimize the absorption effects due to the beryllium slabs and the diamonds of the pressure cell. To achieve this, computer programs (in C language) have been developed that generate optimal setting angles

$(\omega_\psi, \theta_\psi, \varphi_\psi, \chi_\psi)$ of all possible reflections directly from the orientation matrix of the crystal. The ψ settings used were those that minimize the angles, ε_{inc} and ε_{scatt}, formed by the incident and by the diffracted beams with the normal of the gasket plane in the DAC. To partially overcome limiting features of the commercial diffractometer software (viz. XSCANS), single point "ψ-data collections" were made for the angular settings at the best $\psi = 0°$ value, modulo $30°$.

RESULTS

At the pressure 0.3(2) kbar, measured after loading and tightening the diamond anvil cell (DAC) very gently, the cell parameters measured were consistent with those at ambient pressure. In the next step when the pressure had been increased by as small an amount as was reasonable with our current equipment, a pressure of 1.2 kbar was measured. Already at this low pressure, it became apparent that single crystals of triclinic WO₃(II) had undergone a phase transition. Thus, between 0.3 and 1.2 kbar the unit cell changed drastically and a high pressure (HP) form, denoted WO₃(HP), with the dimensions $a = 7.394(2)$, $b = 7.384(2)$, $c = 7.688(3)$ Å, $\alpha = 88.81(3)$, $\beta = 91.20(3)$, and $\gamma = 91.20(3)°$ was formed. These dimensions, when compared to the ambient pressure dimensions, show that the a parameter increased by 0.081 Å ($+ 1.1\%$) and the b parameter decreased by as much as 0.141 Å ($- 1.9\%$). Furthermore, the lattice symmetry changed from being primitive to being C-centered. Transforming the obtained unit cell with

$$T \equiv \begin{pmatrix} 1/2 & -1/2 & 0 \\ 1/2 & 1/2 & 0 \\ 0 & 0 & 1 \end{pmatrix}$$

will then give a primitive monoclinic unit cell with halved unit cell volume. After a least squares refinement with proper monoclinic parameter constraints, the parameters $a = 5.277(1)$, $b = 5.166(1)$, $c = 7.688(2)$ Å, and $\beta = 91.20°$ were obtained. No considerable splitting of the intensity profiles, which would indicate a significant twinning formation during the transition, was observed for the X-ray reflections of the WO₃(HP) form. The phase transition is thus in accordance with the discussion above concluding that, due to the pseudo-C-centering of the triclinic WO₃(II) structure, phases with halved unit cell volumes might be anticipated under nonambient conditions.

No other phase transition was observed when the pressure in the DAC was raised successively up to 47 kbar. Thus, the observed monoclinic WO₃(HP) form appears to be the stable form up to 47 kbar. By releasing the pressure in the pressure cell down to approximately ambient pressure the triclinic form is obtained again, indicating that the monoclinic ↔ triclinic phase transition is reversible. Unfor-

tunately, our current pressure equipment is not suitable for more detailed studies in the low pressure region below a few kbar. Thus, we have not been able to characterize the transition further, with regard to possible hysteresis effects, etc. With the current results, we can only conclude that the transition is reversible and occurs below 1.2 kbar. With regard to the Ehrenfest reaction order (9) of the phase transition, i.e., whether the transition is of discontinuous first-order (possibly with hysteresis) type or of a continuous second-order type, the results are not completely discriminative. However, it appears that the volume changes abruptly at the transition. Further studies of *inter alia* the compressibility of WO₃ at pressures in the range up to 1.2 kbar are clearly needed for a more precise study of the detailed features of the presently described phase transition. A detailed low-pressure study would also yield information if other phase transitions occur, which appears rather plausible. As mentioned before, one of the referees pointed out to us that Salje and Hoppman in 1980 (1) published some high-pressure investigations of WO₃ up to about 14 kbar. Their observations were based on spectroscopic (Raman) and photographic X-ray (Laue) studies. These authors also observed that triclinic WO₃ undergoes a reversible transition at pressures of ≈ 1 kbar to form a monoclinic phase, which they denoted ε-WO₃. The cell dimensions given by Salje and Hoppman, which were obtained from Laue photographs, are in reasonable agreement with those obtained in the present study. Furthermore, a similar phase was reported by Salje *et al.* (10) for specimens with the composition $W_x Mo_{1-x} O_3$. In this phase, the W ions are partially replaced by Mo ions, which might be anticipated to give similar structural effects as those due to an increased external pressure.

To determine the structure of WO₃(HP), single crystal diffraction data were collected at 5.7 kbar, well above the transition pressure. In all, 512 reflections had diffractometer setting angles and a DAC orientation that through a proper choice of the azimuthal angle ψ (cf. above) could enable intensity data to be collected.

The intensity data were first corrected for the absorption in the crystal (see Table 1). This correction was followed by a correction also for the absorption in the DAC hardware. This absorption, or rather decrease in intensity, is frequently a combination of the shadowing of the incident and/or scattered beams by the gasket material and of the absorption in the Be slabs and diamonds of the DAC. It has been shown (11) that these effects are well described using the simple function $\exp[- k \cdot (\varepsilon_{inc}^3 + \varepsilon_{scatt}^3)]$, where ε denotes the angle between the beam and the normal of the gasket plane. The empirical constant k can be obtained from an analysis of a diffraction data set, where each reflection in the set is measured at some different azimuthal angles (giving different values of $\varepsilon_{inc}^3 + \varepsilon_{scatt}^3$). The value of the constant k in the present case was $k = 0.5$ (radian)$^{-3}$.

TABLE 1
Experimental Details of the Structure Determination of the New High Pressure Form WO_3(HP)

Formula	WO_3
Formula weight	231.85
Space group	$P2_1/c$
Unit cell dimensions	$a = 5.261(2)$, $b = 5.128(1)$, $c = 7.650(4)$ Å, and $\beta = 92.05(3)°$
Unit cell volume, V	206.3(1) Å^3
Formula units per unit cell, Z	4
Density (calcd.), d_x	7.46 g cm^{-3}
Radiation (rotating anode)	$MoK\alpha$
Wavelength, λ	0.71073 Å
Temperature, T	293 K
Intensity data collection	ω-2θ scan
Maximum $\sin(\theta)/\lambda$	0.81 Å^{-1}
Internal R	0.059
Collected reflections	512
Unique reflections	252
Observed reflections	227
Criterion for significance	$I \geq 4 \cdot \sigma_I$
Absorption correction	Numerical integration for crystal Semiempirical for pressure cell
Crystal size	$198 \times 136 \times 40$ μm
Linear absorption coefficient	55.7 mm^{-1}
Transmission factor range	0.12 to 0.20
Structure refinement	Full-matrix least squares
Minimised function	$\sum w \cdot (\Delta F)^2$
Anisotropic thermal parameter for	W
Number of refined parameters	24
Weighting scheme	$(\sigma_F^2 + 0.001 \cdot F^2)^{-1}$
R for the observed reflections	0.040
wR for the observed reflections	0.049
Max. of $|\Delta|/\sigma$	< 0.001
Max. and min. of $\Delta\rho$	2.0 and -2.2 e Å^{-3}

Apart from the reasonably low internal R_{int} value (0.059) calculated from monoclinically equivalent reflections, the metric symmetry observed for the unit cell, e.g., α and γ angles refined to values close to 90° (89.95(5)° and 89.95(4)°), can be considered as a further support for using a monoclinic symmetry in the subsequent structure determination of WO_3(HP). The number of symmetry independent reflections with observable intensities ($I > 4 \cdot \sigma_I$) became 227. The systematic extinctions observed among the observed data were consistent with the space group symmetry $P2_1/c$. The choice of the space group symmetry is also supported by the outcome of the structural refinements.

By transforming the fractional coordinates in accordance with the unit cell transformation T given above, it is apparent that the pseudo-symmetry in the triclinic ambient pressure WO_3(II) structure does not deviate much (less than a few hundreds of an Å) from a substructure describable by a monoclinic $P2_1/c$ symmetry and half the unit cell volume. Instead of four independent WO_3 units in the asymmetric unit as in WO_3(II), the monoclinic subcell will contain only one independent formula unit. By modeling the structure

TABLE 2
Fractional Coordinates and Isotropic Displacement Parameters with e.s.d.'s for WO_3(HP) and Anisotropic Displacement Parameters for W

Atom	x	y	z	U_{iso}
W	0.2563(1)	0.2681(1)	0.2882(2)	0.006(1)
O(1)	$-0.042(2)$	0.039(2)	0.202(2)	0.008(2)
O(2)	0.442(2)	$-0.046(2)$	0.199(2)	0.017(3)
O(3)	0.255(3)	0.327(2)	0.012(3)	0.016(2)

U_{11}	U_{22}	U_{33}	U_{23}	U_{13}	U_{12}
0.0052(11)	0.0077(6)	0.0056(24)	$-0.0001(2)$	$-0.0016(13)$	$-0.0004(2)$

with only one anisotropically vibrating atom (W), there will only be 24 parameters needed to describe the most relevant features of the WO_3(HP) structure. The single crystal data collected above the phase transition (5.7 kbar) were used to verify the structure model derived in this way. The structural parameters were refined against the 227 significantly observed reflections to an R value of 0.040 ($wR = 0.049$) The vibrational displacement factors of the atoms have reasonable magnitudes. The U_{iso} values, ranging from 0.006 to 0.017 Å, compare well with those found in the structural investigations of WO_3(II) at ambient pressure (4).

The fractional coordinates and thermal parameters are given in Table 2 and bond distances in Table 3. The coordination around the W atoms with the atomic labels used is shown in Fig. 1. The absolute and relative changes of the unit cell dimensions, determined at 12 different pressures, are listed in Table 4. The relative changes in unit cell parameters are shown in Fig. 2.

TABLE 3
W–O Distances with e.s.d.'s in Parentheses in the Distorted Coordination Octahedra of the New High Pressure WO_3(HP) Phase at 5.7 kbar (Present Study), and in the Four Crystallographically Independent Ones (e.s.d.'s ≈ 0.02Å) of Triclinic WO_3(II) at Ambient Pressure (4)

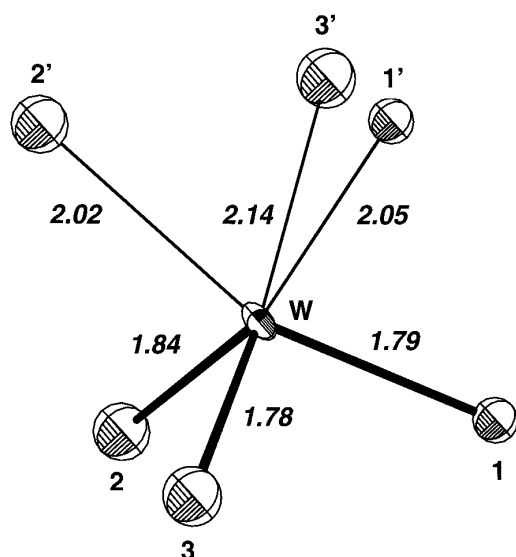| Monoclinic HP form at 5.7 kbar (Å)		Triclinic WO_3(II) at ambient pressure			
		W(1) (Å)	W(2) (Å)	W(3) (Å)	W(4) (Å)
W–O(3)	1.78(2)	1.75	1.77	1.71	1.74
O(1)	1.79(1)	1.75	1.79	1.80	1.75
O(2)	1.85(1)	1.83	1.85	1.86	1.88
O(2′)	2.02(1)	1.95	1.92	1.98	1.94
O(1′)	2.05(1)	2.06	2.12	2.08	2.05
O(3′)	2.14(2)	2.21	2.20	2.17	2.15

FIG. 1. Oxygen coordination around the tungsten atoms in the monoclinic high-pressure form, WO₃(HP), showing bond distances and atomic labeling. The primed labels indicate that the positions are generated by applying the crystallographic symmetry.

The refinements of structural models were performed with the SHELXTL program package, using atomic scattering factors for neutral atoms collected from the International Tables of Crystallography (12). The program ATOMS (13) was utilized to obtain the structure diagrams.

DISCUSSION

The W atoms in triclinic WO₃(II) and in monoclinic WO₃(HP) are octahedrally coordinated by oxygen atoms. These coordination octahedra share all six corners with adjacent octahedra to form a three-dimensional structure (cf. Fig. 3). The symmetry of an ideal arrangement of this type would of course be cubic (ReO₃ structure type). However, in both WO₃ phases adjacent bonds in linear –O–W–O–W–O– arrangements have alternating lengths of ≈ 1.8 and ≈ 2 Å, respectively. and O–W–O and W–O–W bond angles that deviate significantly from 0°, modulo 90°.

Although the overall geometrical features of the atomic arrangements are similar both in WO₃(II) and in WO₃(HP), the coordinations around the W atoms differ. The W–O bond lengths in the distorted coordination octahedra of WO₃(HP) are in increasing order 1.78(2), 1.79(1), and 1.85(1) Å for the three shorter bonds and 2.02(1), 2.05(1), and 2.14(2) Å for the three longer ones. Thus the W atoms in WO₃(HP) can be considered as being 3 + 3 coordinated, with a separation of 0.17 Å between the two groups of bond lengths. The averages of the corresponding values in the ambient pressure WO₃(II) phase are 1.74, 1.77, 1.85, 1.94, 2.08, and 2.18 Å, respectively. Accordingly, in WO₃(II) there

are four shorter bonds (< 2.0 Å) and two longer bonds with a separation of 0.14 Å between the groups. The four oxygen atoms forming the shorter bonds give a distorted tetrahedral coordination, with the remaining two oxygen atoms capping the tetrahedra. Such tetrahedra form chains (14) through corner sharing that extend along [1 0 0]. In WO₃(HP) on the other hand, the oxygen atoms forming the three shorter bonds are all on one side of the W atom. The W atom and three oxygen atoms form isolated pyramids in the structure. Another difference is the deviations of the W positions between the two WO₃ phases. The different W arrangement is obvious when, e.g., viewing the W positions in the two structures along [001] as in Fig. 4.

In the structures of both WO₃(II) and WO₃(HP), the W positions show displacements out off the centroids of the coordination octahedra. These off-center displacements

TABLE 4
Compressibility Data for WO₃(HP) with e.s.d.'s Are in Parentheses

	Absolute values				
P	a (Å)	b (Å)	c (Å)	β (Å)	V (Å³)
0	5.289	5.203	7.690		211.5
1.2	5.277(1)	5.166(1)	7.688(2)	91.67(2)	209.5(1)
2.6	5.271(2)	5.154(1)	7.671(4)	91.81(3)	208.3(1)
3.6	5.267(3)	5.141(2)	7.668(5)	91.93(4)	207.5(1)
5.7	5.261(2)	5.128(1)	7.650(4)	92.05(3)	206.3(1)
9.9	5.253(3)	5.100(1)	7.641(7)	92.30(6)	204.5(2)
14.8	5.242(3)	5.070(2)	7.620(6)	92.58(6)	202.3(2)
20.0	5.238(3)	5.045(2)	7.589(5)	92.78(4)	200.3(1)
24.7	5.230(5)	5.019(2)	7.576(9)	93.03(8)	198.6(2)
31.8	5.222(3)	4.988(6)	7.518(10)	93.55(8)	195.5(3)
36.4	5.212(2)	4.966(3)	7.508(7)	93.69(6)	193.9(2)
40.5	5.209(1)	4.945(2)	7.487(4)	93.72(3)	192.5(1)
47.1	5.203(1)	4.917(3)	7.444(9)	94.31(4)	189.9(2)

	Relative values			
P	a (Å)	b (Å)	c (Å)	V (Å)
1.2	1.000	1.000	1.000	1.000
2.6	0.999(1)	0.997(1)	0.998(1)	0.994(1)
3.6	0.998(1)	0.995(1)	0.997(1)	0.990(1)
5.7	0.997(1)	0.993(1)	0.995(1)	0.984(1)
9.9	0.996(1)	0.987(1)	0.994(2)	0.976(2)
14.8	0.993(1)	0.981(1)	0.991(2)	0.965(2)
20.0	0.992(1)	0.977(1)	0.987(1)	0.956(1)
24.7	0.991(2)	0.971(1)	0.985(2)	0.948(2)
31.8	0.989(1)	0.965(2)	0.978(2)	0.933(3)
36.4	0.988(1)	0.961(1)	0.976(2)	0.925(2)
40.5	0.987(1)	0.957(1)	0.974(1)	0.919(1)
47.1	0.986(1)	0.952(1)	0.968(2)	0.906(2)

Note. The e.s.d.'s of the measured pressures are estimated to 0.3 kbar. The cell parameters for 0 kbar were estimated by applying the proper transformation (cf. text) to the precise parameters obtained by Woodward *et al.* (2) for the triclinic phase.

FIG. 2. (a) Relative changes of the unit cell parameters (cf. Table 4) of $WO_3(HP)$. (b) Relative volume changes calculated with the fitted Birch equation of state (solid line) and the observed volume changes (filled circles). The equation was derived from data at pressures above 3.6 kbar.

might possibly be regarded as "displacive modulations" running through the structure. The displacement directions are roughly along $\pm [021]$ in triclinic $WO_3(II)$ and roughly along the $\pm [001]$ direction in $WO_3(HP)$ (cf. Fig. 5), and they are arranged in an antiparallel fashion. These off-center displacements can thus be considered as becoming almost

one-dimensional after the phase transition that leads to the $WO_3(HP)$ form.

The three symmetry independent bridging W–O–W angles between the coordination octahedra are 155.0°, 145.0°, and 156.0° for the oxygen atoms O(1), O(2), and O(3), respectively. In triclinic $WO_3(II)$ the average of the W–O–W
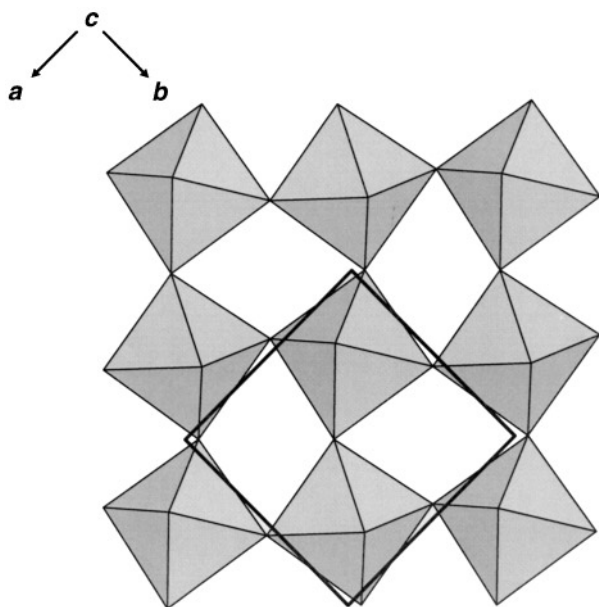
FIG. 3. Polyhedral representation of the structure of the high-pressure phase WO$_3$(HP), viewed along [001].

angles is 157.8°. The smaller average of the W–O–W angles in WO$_3$(HP) indicates that a more tilted arrangement of the coordination octahedra is formed with the phase transition.

The O–W–O bond angles involving adjacent oxygen atoms in the coordination octahedra of WO$_3$(HP) range from 76.2° to 98.5°. As might be expected from simple sterical reasons the smaller angles (76.2° to 78.9°) are encountered between the three longer W–O bonds and the larger

angles (97.1° to 98.5°) between the three shorter W–O bonds. In the first case the O ··· O distances are around 2.6 Å and in the latter case they are around 2.7 Å.

Bond valence sum (bvs) values estimated with the parameters derived by Brown and Altermatt (15) are 2.1, 2.0, and 2.0 valence units for the three symmetry independent oxygen atoms O(1), O(2), and O(3), respectively. For the W atom, the bvs value becomes 6.1 valence units. Thus, the estimated bvs values are all in agreement with the individual formal charges.

The variation of the unit cell dimensions for WO$_3$(HP) with pressure (cf. Fig. 2a) show that the compressibility is not entirely isotropic. The compressibility along [010] is larger than that along the other axes. The observed unit cell volumes versus pressure (cf. Fig. 2b) have been fitted through a least squares procedure to the Birch-type equation of state (16), which is computationally simpler to handle than the rather equivalent (17) Murnaghan-type equation (18). The coefficients B_0 and B_0' in the Birch equation

$$P = 3/2 \cdot B_0(x^{-7/3} - x^{-5/3})(1 - 3/4 \cdot (4 - B_0')(x^{-2/3} - 1)),$$

where B_0 is the isothermal bulk modulus at ambient pressure and B_0' is its derivative with respect to P at ambient pressure, were determined to be 44.5(9) and 2.5(4) GPa respectively. In the equation x denotes the volume ratio V/V_0 and P the observed pressure. Due to the large correlation between B_0 and B_0', the marginal e.s.d.'s quoted are somewhat unreliable. The experimental data, in the range 3–47 kbar, are well represented by the Birch equation. This fact might be taken as a further verification that the
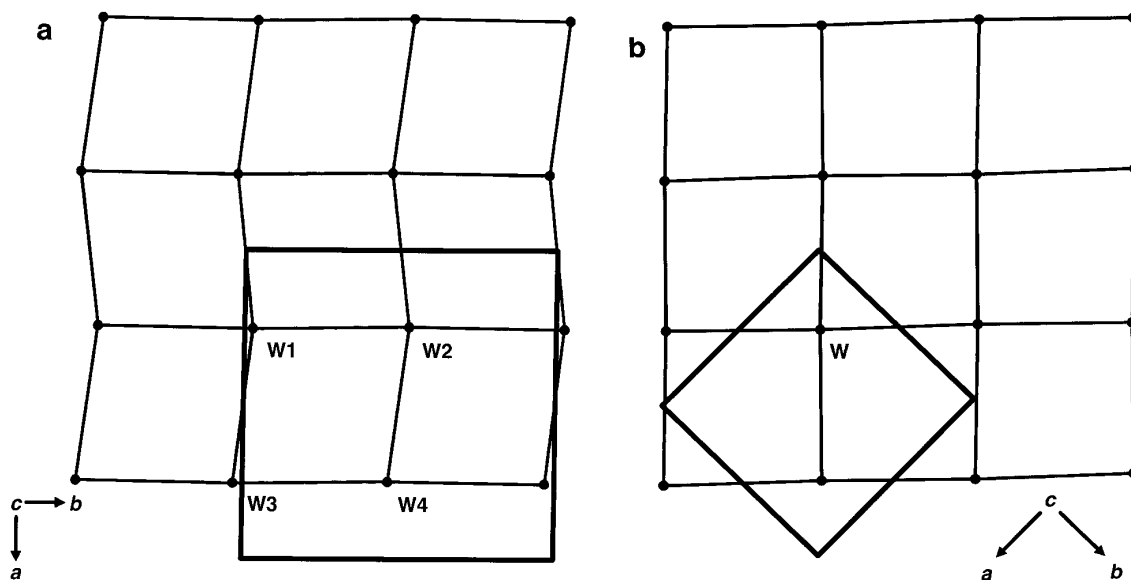

FIG. 4. The W arrangement in WO$_3$. For clarlity, the W atomic positions have been connected by thin lines. (a) The triclinic WO$_3$(II) phase (ambient pressure). (b) The monoclinic high-pressure phase WO$_3$(HP).
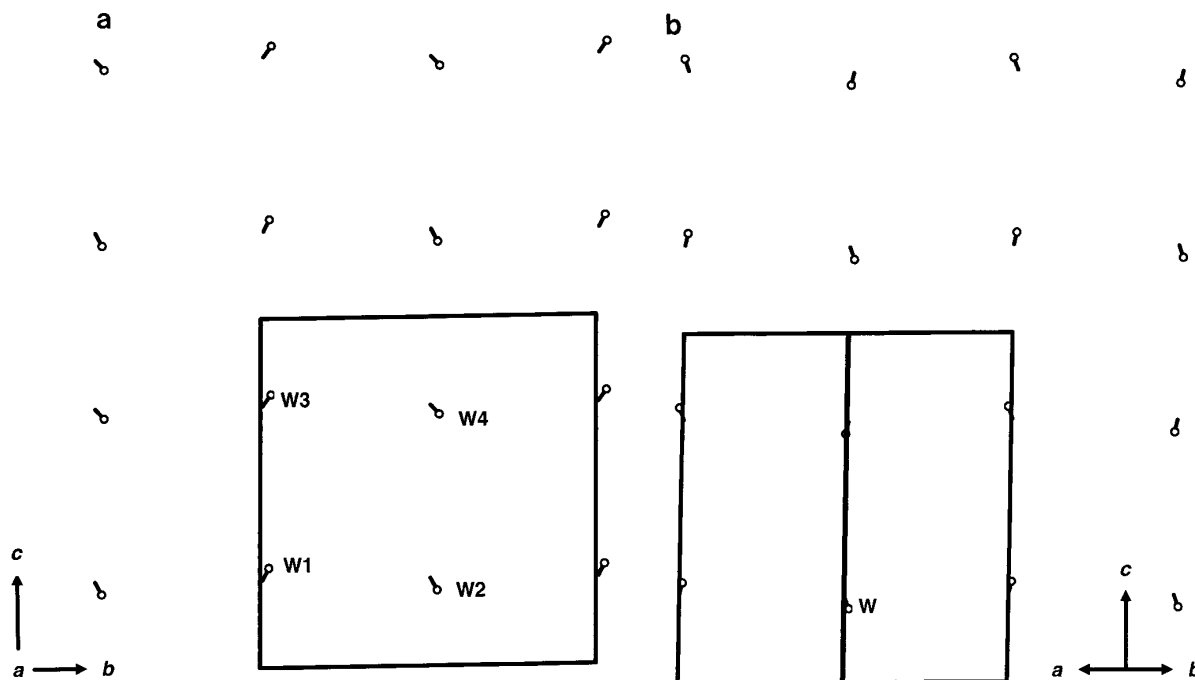
FIG. 5. The displacements of the W atoms out of the coordination octahedra. The ends of the short lines marked with unfilled cricles denote the W positions while the other ends of the lines show the centroid positions. (a) The triclinic $WO_3(II)$ phase (ambient pressure) viewed along [100] of the triclinic cell. (b) The monoclinic high-pressure phase $WO_3(HP)$ viewed along [110] of the monoclinic cell.

compressibility data do not contain information on any phase transition in the investigated pressure range. The bulk modulus is *inter alia* expected to increase with increasing cation charge and to decrease with increasing ionic radius. For MoO_3, the cation has the same formal charge but a slightly larger radius, 0.73 Å for Mo^{6+} compared to 0.60 Å for W^{6+} (19). The bulk modulus determined for MoO_3 is smaller, 32.0(9) GPa (20), and thus follows the expected trend. However, the larger softness of MoO_3 is most probably due to its layer-type structure.

In view of the known complexity of structures and phase transitions of WO_3 as a function of temperature, leading to *inter alia* the existence of phases with symmetries that increase with temperature, one might anticipate more transitions to occur also at higher pressures. Eventually one could anticipate the WO_3 with an ideal cubic ReO_3 structure type will be obtained. Studies of single crystalline WO_3 at pressures above 50 kbar are currently being planned.

REFERENCES

1. E. Salje and G. Hoppman, *High Temperature High Pressure* **12,** 213–216 (1980).
2. P. M. Woodward, A. W. Sleight, and T. Vogt, *J. Phys. Chem. Solids* **56,** 1305–1315 (1995).
3. E. Salje, *Ferroelectrics* **12,** 215–217 (1976).
4. Diehl, Brandt and E. Salje, *Acta Crystallogr. Sect. B* **34,** 1105–1111 (1978).
5. Ph. Labbe, *in* "Diffusionless Phase Transitions and Related Structures in Oxides" (C. Boulesteix, Ed.). Trans Tech Publications Ltd. Zürich, 1992.
6. H. Braekken, *Z. Krist.* **78,** 484–489 (1931).
7. Y. Xu, S. Carlson, and R. Norrestam, *Acta Crystallogr. Sect. A* **52,** 536 (1996).
8. G. J. Piermarini, B. Block, J. D. Barnet, and R. A. Forman, *J. Appl. Phys.* **46,** 2774–2780 (1975).
9. P. Ehrenfest, *Proc. Acad. Sci. Amsterdam* **36,** 153–157 (1933).
10. E. Salje, R. Gehlig, and K. Viswanathan, *J. Solid State Chem.* **25,** 239–250 (1978).
11. R. Norrestam, to be published, 1977.
12. "International Tables for X-Ray Crystallography," Vol. IV, Kynoch, Birmingham, 1974.
13. E. Dowty, "*ATOMS*, A Computer Program for Displaying Atomic Structures." 521 Hidden Valley Road, Kingsport, TN 37663, 1989.
14. L. Kihlborg, *Ark. Kemi* **21,** 357–364 (1963).
15. I. D. Brown and D. Altermalt, *Acta Crystallogr. Sect. B* **41,** 244–247 (1985).
16. F. Birch, *J. Geophys. Res.* **57,** 227 (1952).
17. O. L. Anderson, *J. Phys. Chem. Solids* **27,** 547–565 (1966).
18. F. D. Murnaghan, *Proc. Natl. Acad. Sci.* **30,** 244 (1944).
19. R. D. Shannon, *Acta Crystllogr. Sect. A* **32,** 751–767 (1976).
20. Y. Xu, S. Carlson, and R. Norrestam, to be published, 1997.